Electronic Supplementary Material (ESI) for Inorganic Chemistry Frontiers

Supporting information

Sandwich-like Carbon-anchored Ultrathin TiO_2 Nanosheets Realizing Ultrafast Lithium Storage

Yongfu Sun[1,†], Jinbao Zhu[1,†], Liangfei Bai[1], Qiuyang Li[1], Xing Zhang[1], Wei Tong[2] and Yi Xie[1,*]

[1] Hefei National Laboratory for Physical Sciences at Microscale, Collaborative Innovation Center of Chemistry for Energy Materials, University of Science & Technology of China, Hefei, Anhui 230026, (P.R. China), E-mail: yxie@ustc.edu.cn.

[2] High Magnetic Field Laboratory, Chinese Academy of Sciences, Hefei, Anhui, 230031, P.R. China.

[†]These authors contributed equally to this work

S1. Experimental Section

Preparation of samples: In a typical experiment, 1 mL hexafluorotitanic acid was first added to 30 mL isopropanol to form the hexafluorotitanic acid-isopropanol solution. Then 2 mL octylamine was slowly dropped to the stirring solution before being transferred to a Telflon-lined stainless steel autoclave and then heated in an electric oven at 180 °C for 24 h. After reaction, a white powder was obtained by centrifugation, washed with ethanol and water several times, and then dried in vacuum at 60 °C overnight. Finally, the sandwich-like carbon-delaminated TiO_2 nanosheets were prepared by pyrolysis as-obtained layered organic-inorganic nanosheets in 450 °C for 2 h in Ar flow.

Characterization： X-ray powder diffraction (XRD) patterns were recorded by using a Philips X'Pert Pro Super diffractometer with Cu Kα radiation (λ=1.54178 Å). The transmission electron microscopy (TEM) images were obtained by a Hitachi Model H-7650 instrument with a tungsten filament. High-resolution transmission electron microscopy (HRTEM) images and electron diffraction (ED) patterns were carried out on a JEOL-2010 transmission electron microscope at an acceleration voltage of 200 kV. Raman spectra were recorded at ambient temperature with a LABRAM&HR Confocal Laser Micro Raman Spectrometer. The nitrogen adsorption-desorption isotherms and corresponding pore size distribution were measured using a Micromeritics ASAP 2000 system at 77 K. Thermogravimetric analysis was determined using a thermal gravity analyzer (TGA) at a temperature rise rate of 10 °C/min from room temperature to 600 °C under a continuous air flow. For ^{13}C and ^{1}H CP/MAS or magic angle spinning (MAS) NMR measurements were obtained with a 500.132 MHz NMR spectrometer (Bruker, Germany) at 298 K. The infrared spectra were measured on a NICOLET Fourier transform infrared spectrometer, using pressed KBr tablets. AC electrochemical impedance measurements were performed using electrochemical station at room temperature (CHI660B).

Electrochemical measurements： The electrochemical measurements were carried out using home-made button cells with lithium metal as the counter and reference

electrodes at room temperature. The electrode consisted of active material, conductivity agent (acetylene black), and polymer binder (polyvinylidene difluoride, PVDF) by a weight ratio of approximately 80:10:10. The dried material was coated on a copper foil and dried in a vacuum oven at 110 °C for 10 h, the active materials loading in each electrode was typically about 2 mg. The electrolyte was 1 M $LiPF_6$ in a 50:50 V/V mixture of ethylene carbonate/dimethyl carbonate (EC/DMC), and a microporous membrane (Celguard 2400, USA) as the separator. Cell assembly was carried out in an Ar-filled glove box and galvanostatic charge–discharge cycling performance was conducted at different current densities with a fixed voltage window between 3 V and 1V.

S2. TEM images for bare TiO_2 nanosheets

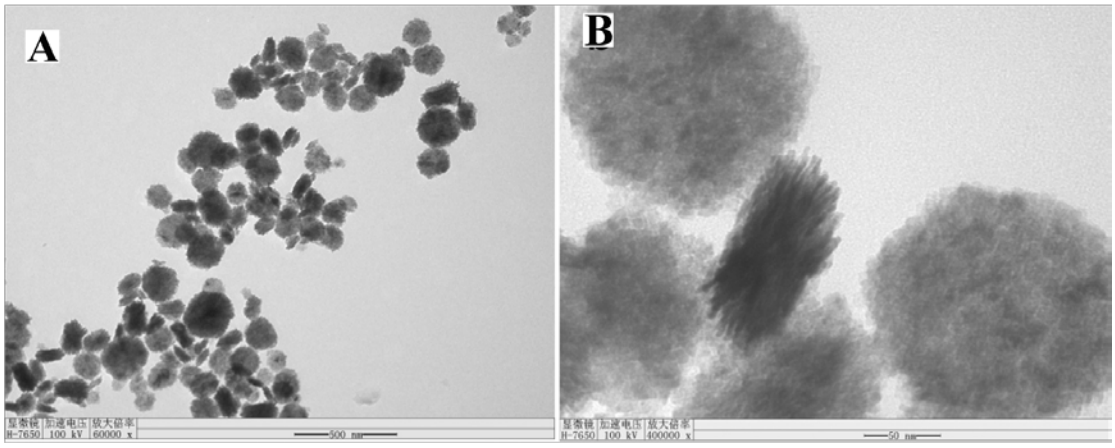

Figure S1. TEM images of bare TiO_2 nanosheets prepared at the low concentration of octylamine.

S3. FT-IR spectrum of lamellar TiO_2-octylamine hybrid nanosheets

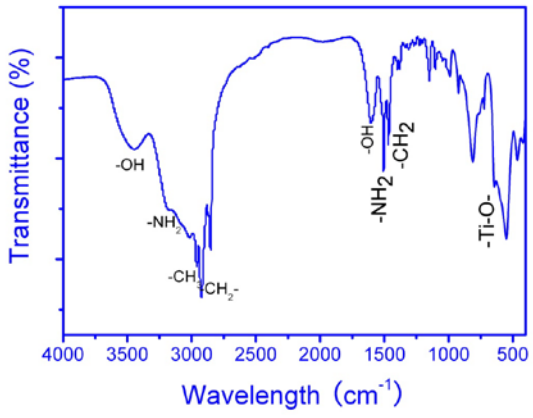

Figure S2. FT-IR spectrum of the lamellar TiO_2-octylamine hybrid nanosheets.

The presence of octylamine in the lamellar TiO_2-octylamine hybrid nanosheets was also confirmed by the FT-IR spectrum in Figure S2, which displays OH stretching (3464, 1591cm^{-1}) modes, CH_2 bending (1447, 2863 cm^{-1}) and CH_3 stretching (2921, 2972 cm^{-1}) modes. The broad peak sat around 3200 cm^{-1} and 1480 cm^{-1}, corresponding to the NH_2 stretching mode, mean that the interlayer organic molecules were intercalated as ammonium cations instead of neutral amines.[1] In addition, IR absorption peaks at around 500 cm^{-1} could be assigned as Ti-O lattice vibrations as found in TiO_2. These results give strong evidence for the formation of lamellar TiO_2-octylamine hybrid nanosheets.

S4. Raman spectrum and TGA profile of carbon-anchored ultrathin TiO_2 nanosheets

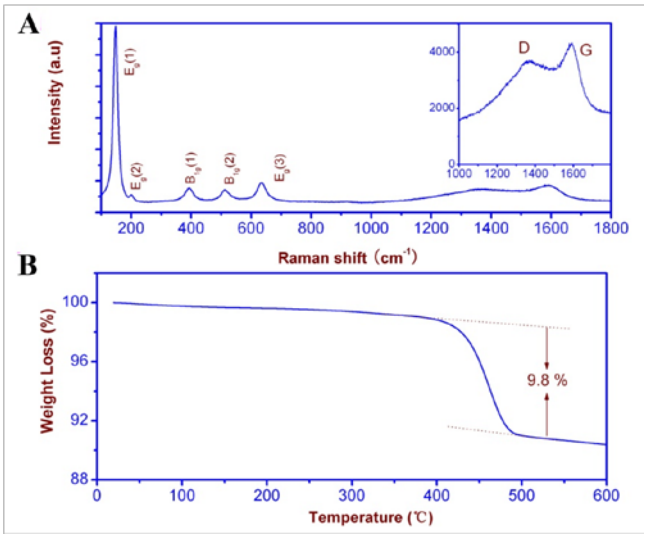

Figure S3. (A) Raman spectrum and (B) TGA analysis for the sandwich-like carbon-anchored ultrathin TiO_2 nanosheets.

As shown in Figure S3A, Raman spectrum of the sandwich-like carbon-anchored ultrathin TiO_2 nanosheets was performed to test the presence of anatase TiO_2 and carbon. The typical five Raman modes around 100-800 cm^{-1} were confirmed to anatase TiO_2 without any undesirable polymorphs detected.[2] Interestingly, there are two peaks at 1339 and 1603 cm^{-1} in Raman spectrum, which indicate the existence of carbon coating layer, originating from disordered and ordered graphitic carbon.[3] It was generally accepteded that the ratio between the D and G band was found to correlate to the nature of carbon; in the present case, the dimensional ratio of the G

band to the D band for CRTNs was estimated to be about 1.39, which indicated the formation of a reasonable degree of graphitization.[4] Thermo-gravimetric analysis (TGA) was carried out to confirm the amount of carbon in the sandwich-like carbon-anchored ultrathin TiO_2 nanosheets, the trival weight loss before 400 °C could be ascribed to surface water adsorption, the weight loss after 400 °C could be ascribed to carbon oxidation, and the weight fraction of carbon in the resulting nanosheets was about 9.8% (Figure S3B).

S5. Nitrogen physisorption measurements of carbon-anchored ultrathin TiO_2 nanosheets and bare TiO_2 nanosheets

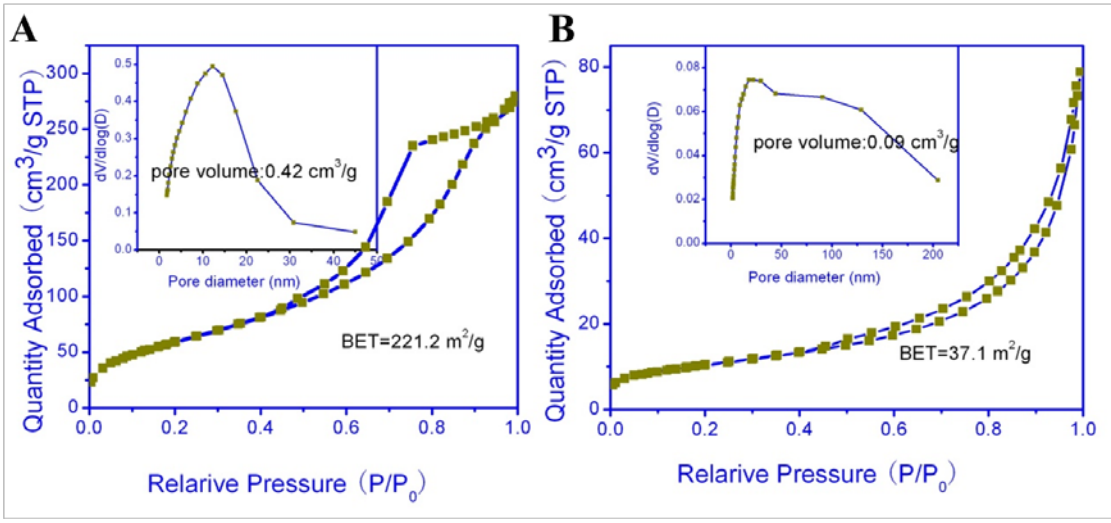

Figure S4. The N_2 adsorption-desorption isotherms and corresponding pore size distribution of (A) carbon-anchored ultrathin TiO_2 nanosheets and (B) bare TiO_2 nanosheets calculated by Barretl-Joyner-Halenda (BJH) method from desorption branch.

The specific surface areas and porous nature of the carbon-anchored ultrathin TiO_2 nanosheets and bare TiO_2 nanosheets were further investigated by nitrogen adsorption/desorption measurements conducted at 77 K. The isotherms of carbon-anchored ultrathin TiO_2 nanosheets can be classified as type IV isotherms, revealing that the material is composed of aggregates (loose assemblages) of sheet-likenanostructures forming slit-like pores.[5] The as-obtained carbon-anchored ultrathin TiO_2 nanosheets have a huge BET surface areas of 221.2 m^2/g with a pore volume of 0.42 cm^3/g (Figure S4A), higher than previously reported values of TiO_2 nanostructures and inorganic graphene analogues.[6] However, the specific surface

area of bare TiO_2 nanosheets is only 37.1 m^2/g with irregular pore diameter and a pore volume of 0.09 cm^3/g (Figure S4B). The low surface areas of nanoparticles should be attributed to the larger crystal size resulting from aggregation in preparation.

S6. Solid-state ^{13}C and ^{1}H NMR spectra

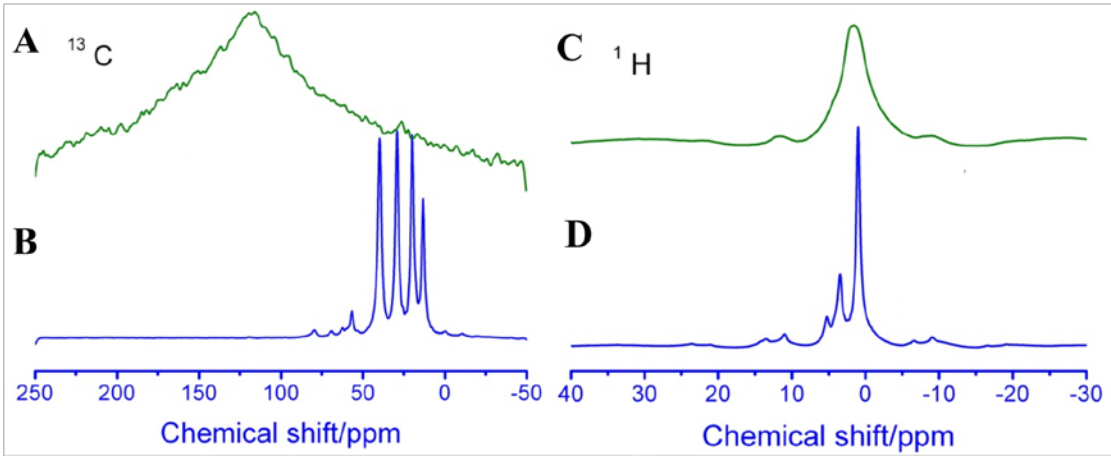

Figure S5. Cross polarization/magic angle spinning (CP/MAS) solid state ^{13}C nuclear magnetic resonance (NMR) spectra of (A) carbon-anchored ultrathin TiO_2 nanosheets and (B) lamellar TiO_2-octylamine hybrid nanosheets; magic angle spinning (MAS) solid state ^{1}H NMR spectra of (C) carbon-anchored ultrathin TiO_2 nanosheets and (D) lamellar TiO_2-octylamine hybrid nanosheets.

Solid-state ^{13}C and ^{1}H NMR spectra were employed to support the proposed mechanism (Figure S5). The organic carbon component in the intercalated octylamine layers can be identified using the cross polarization/magic angle spinning (CP/MAS) solid state ^{13}C NMR spectrum (Figure S5A). a distinct ^{13}C singal is observed around 120 ppm, lack of C-H dipolar and C-C J-dephasing, revealing the formation of orthocarbonate bands.[7] Taken the Raman results into consideration, we identify that the orthocarbonate centers are incorporated into the TiO_2 lattice through the formation of Ti-O-C bonds. In general, it is anticipated that the removal of octylamine layers will lead to complete condensation of the layered titanate structure during the annealing processes at 450 °C. However, the MAS solid state ^{1}H NMR spectrum (Figure S5B) shows that these organic components are partially carbonized at 450 °C *in-situ*, due to the strong bonding force between the titanate and organic layers. This provides strong evidence for the formation of nanocarbons.

S7. XPS spectra of carbon-anchored ultrathin TiO_2 nanosheets

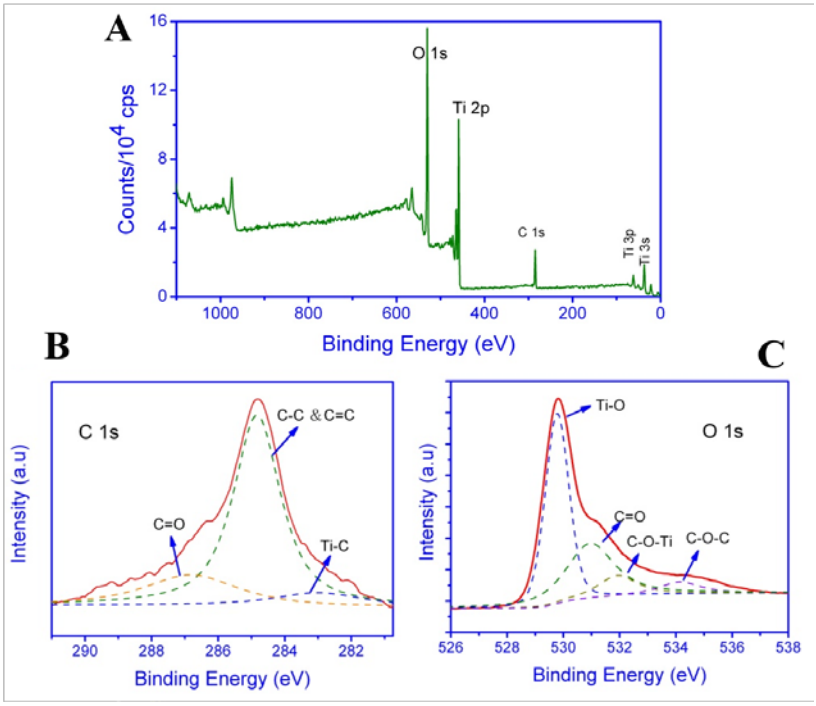

Figure S6. (A) Survey XPS spectrum of the as-obtained carbon-anchored ultrathin TiO_2 nanosheets. (B, C) High-resolution XPS spectra of C 1s and O 1s, respectively; the binding energies found using XPS are corrected for specimen charging by referencing the C 1s line to 284.8 eV.

The binding between the carbon and ultrathin reduced TiO_2 nanosheets was studied by X-ray photoelectron spectroscopy (XPS). The XPS survey spectrum reveals that the as-obtained sample only consists of the elements Ti, O and C (Figure S6A), which is consistent with our analysis mentioned above. The deconvoluted peak centered at 284.8 eV was assigned to the C–C and C=C bonds (Figure S6B). Furthermore, the peak centered at about 286.8 eV was attributed to the C=O and/or O–C=O bonds;[8] the deconvoluted peak centered at 283.4 eV was attributed to the formation of Ti-C bond at this annealing temperature.[9] The results obtained from the XPS analysis also suggest presence of Ti-O-C carbonaceous bonds within the sample annealed at 450 °C, which was further supported by the high-resolution XPS spectra of O 1s. it contains multiple components due to the coexistence of different chemical states of oxygen (Figure S6C). It can be deconvoluted into four peaks: the peaks at binding energies of 529.8, 531.0, 531.8 and 534.1 eV can be attributed to the Ti-O, C=O, C-O-Ti and C-O-C bonds, respectively.[9b, 10]

S8. TEM images of carbon-anchored ultrathin TiO_2 nanosheets before and after cycling

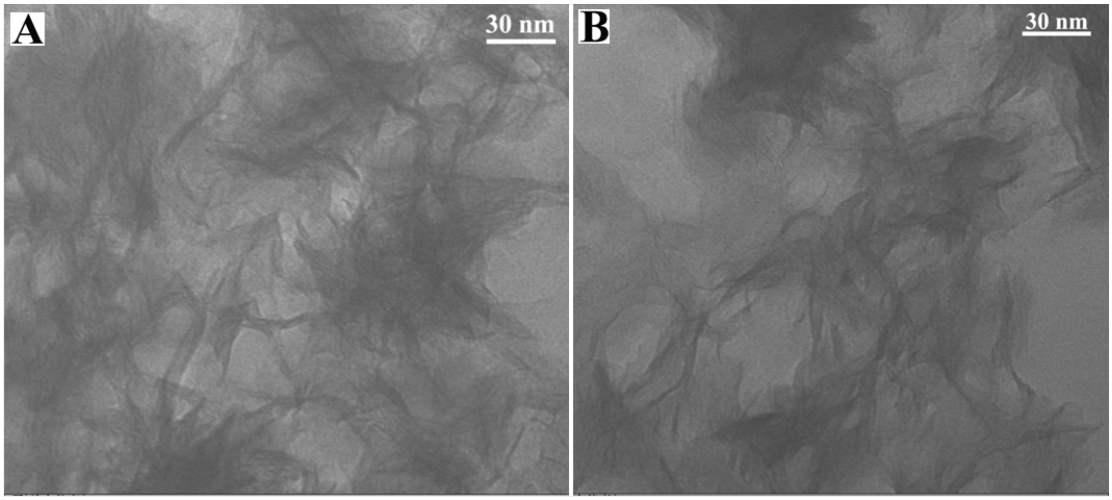

Figure S7. TEM images for the sandwich-like carbon-anchored ultrathin TiO_2 nanosheets (A) before and (B) after 1200 cycles at a constant current drain of 5 C (1 C=170 mA/g).

References

[1] K. Kai, Y. Yoshida, Y. Kobayashi, H. Kageyama, G. Saito, *Dalton T* **2012**, *41*, 825-830.

[2] X. B. Chen, L. Liu, P. Y. Yu, S. S. Mao, *Science* **2011**, *331*, 746-750.

[3] X. Zhang, Z. Xing, L. L. Wang, Y. C. Zhu, Q. W. Li, J. W. Liang, Y. Yu, T. Huang, K. B. Tang, Y. T. Qian, X. Y. Shen, *J Mater Chem* **2012**, *22*, 17864-17869.

[4] L. C. Liu, Q. Fan, C. Z. Sun, X. R. Gu, H. Li, F. Gao, Y. F. Chen, L. Dong, *J Power Sources* **2013**, *221*, 141-148.

[5] C. Wang, Y. Zhou, M. Y. Ge, X. B. Xu, Z. L. Zhang, J. Z. Jiang, *J Am Chem Soc* **2010**, *132*, 46-47.

[6] a.I. Moriguchi, R. Hidaka, H. Yamada, T. Kudo, H. Murakami, N. Nakashima, *Adv Mater* **2006**, *18*, 69-73; b. J. C. Yu, G. S. Li, X. C. Wang, X. L. Hu, C. W. Leung, Z. D. Zhang, *Chem Commun* **2006**, 2717-2719; c. J. M. Li, W. Wan, H. H. Zhou, J. J. Li, D. S. Xu, *Chem Commun* **2011**, *47*, 3439-3441; d. J. T. Jang,

S. Jeong, J. W. Seo, M. C. Kim, E. Sim, Y. Oh, S. Nam, B. Park, J. Cheon, *J Am Chem Soc* **2011**, *133*, 7636-7639; e. J. W. Seo, Y. W. Jun, S. W. Park, H. Nah, T. Moon, B. Park, J. G. Kim, Y. J. Kim, J. Cheon, *Angew Chem Int Edit* **2007**, *46*, 8828-8831.

[7] E. M. Rockafellow, X. Fang, B. G. Trewyn, K. Schmidt-Rohr, W. S. Jenks, *Chem Mater* **2009**, *21*, 1187-1197.

[8] a. C. Y. Yen, Y. F. Lin, C. H. Hung, Y. H. Tseng, C. C. Ma, M. C. Chang, H. Shao, *Nanotechnology* **2008**, *19*; b. O. Akhavan, M. Abdolahad, Y. Abdi, S. Mohajerzadeh, *Carbon* **2009**, *47*, 3280-3287.

[9] a. L. C. Chen, Y. C. Ho, W. S. Guo, C. M. Huang, T. C. Pan, *Electrochim Acta* **2009**, *54*, 3884-3891; b. O. Akhavan, R. Azimirad, S. Safa, M. M. Larijani, *J Mater Chem* **2010**, *20*, 7386-7392.

[10] G. M. Zhou, D. W. Wang, L. C. Yin, N. Li, F. Li, H. M. Cheng, *Acs Nano* **2012**, *6*, 3214-3223.